PEelse: a 2D parallel spectral code for linear elastic analysis of seismic wave propagation

Implementation of seismic sources (plane wave and seismic moment tensor), absorbing boundaries and damping factor

F. Maggio, L. Massidda and M. Stupazzini

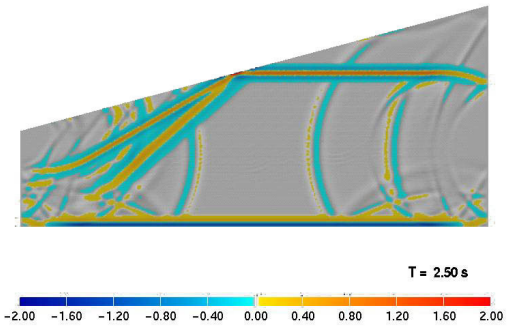

1 Introduction

PEelse2D is a spectral element, parallel, computer program for the analysis of complex 2D structure system, subject to transient dynamic loading conditions. PEelse2D is developed by the CRS4 team (CM4E - SSM area - F.Maggio, L. Massidda, G. Siddi and J.Sabadelle).

The co-operation between the CRS4 and the Technical school of Milan (Department of Structural Engineering) is intended to equip the program of typical tools necessary for the simulation of seismic wave propagation into linear visco-elastic medium.

The goal of the present report is to present the results obtained during the period 15 July – 14 September 2002, on three important topics:

- portability of PEelse2D;
- functionality of PEelse2D;
- implementation of the necessary tools for the analysis in the seismic wave field:
  - most common sources in the seismic field (plane wave in the form of Ricker wavelet and seismic moment tensor (Madariaga, 1983));
  - internal soil dissipation as described by Kosloff and Kosloff (1986);
  - Absorbing boundaries condition (Stacey, 1988).

The term *portability* and *functionality* are intended to describe, respectively, the possibility of the program to be re-compiled and executed outside the CRS4, while the latter and running the entire simulation (pre-processing – analysis – post-processing) in a reduced period.

2 PEelse2D – program characteristics

PEelse2D is a parallel program, based on a purely spectral decomposition scheme of 2D computational domain; the chosen program formulation is defined "element by element". This is due to results of numerical tests according to which, this particular formulation performs better on huge problems (nodes number greater than ~ 10^4) than the "assembled matrix" approach.

The program presents the following characteristics:

- material type: linear elastic (no damping provided);
- boundary conditions: Neumann and Dirichlet;
- loading conditions: point load force, with time history shape of Ricker wavelet ("β" or "*cos*" type) or force time history provided by the user.

PEelse2D is written in Fortran 90 and adopts the external libraries Aztec and Metis. Aztec is a parallel iterative library for solving linear systems (http://www.cs.sandia.gov/CRF/aztec1.html) and Metis is a family of programs for partitioning unstructured graphs and grids (http://www-users.cs.umn.edu/~karypis/metis/metis/ download.html). Both libraries represent in our view the state-of-the-art algorithm on parallel computers and can be freely downloaded. This choice is related with the primary goal of PEelse2D: provide a computer program easy to use for engineering applications and, at the same time, characterised by high performance in terms of efficiency and solution accuracy.

3 Program portability and functionality

First test performed is related with the capability of PEelse2D of concluding an entire analysis in a short period, with the hardware and software available at the Technical School of Milan.

It is important to mention that all results presented in this report are performed, from the pre-processing step (mesh generation with PATRAN 2001 MSC) to the analysis, on two computers located on Milan (OS Linux Suse 8.0 on both computers; first computer: AMD Duron 850MHz with 512 Mb RAM; second computer: AMD Athlon 1800 Xp, with 512 Mb RAM).

The portability and the functionality of PEelse2D are both deeply explored and tested by the number of simulation performed. Finally it is recognised that PEelse2D satisfies well both requirements of fast solver for seismic engineering problems and easy-to-use software.

3.1 Mesh generation (pre-processing)

The mesh generation process is performed thanks to the commercial software MSC-Patran 2001 (Linux version), available at the Technical School of Milan. The translation of Patran output format in PEelse2D input format is obtained with a specific program, created by the CRS4 team in Python language.

3.2 Numerical analysis

Simulation run are performed compiling PEelse2D on the CRS4 computers. The executable file is uploaded at Milan computers and then simulations are performed on them.

3.3 Results analysis (post-processing)

Finally the post-processing is carried on a mobile computer (Pentium III, 256 Mb) with Windows OS. The graphical visualisation of the results, consisting on time-history on chosen nodes and snapshot at decided simulation time, is conducted with the commercial software Mathworks-Matlab v6.0 and free software MayaVi v1.2 (http://mayavi.sourceforge.net).

4 Most important advantages of PEelse2D

Thanks to the work developed at the CRS4 is now possible underline at least two important characteristics of PEelse2D simulation process:

- great advantages in terms of flexibility on pre-processing phase: mesh generation is very simple and the possibility of adopting MSC-Patran is fully explored. Spectral integration nodes (Legendre-Gauss-Lobatto nodes) are created inside PEelse2D and this allows an important reduction of time spent in mesh generation process against AHNSE (Casadei e Gabellini, 1988).
- Time analysis (seconds per time step) is just like the same of ELSE (Faccioli et al., 1997), in spite of the fact that PEelse2D allows unstructured mesh and parallel runs.

5 Plane wave source

We have dedicated to plane wave source implementation on PEelse2D and an extensive test phase. The plane wave source is intended to be SV and P wave, travelling in the y axes direction (like Fig. 1).

Plane wave source is realised introducing a force time history, able to generate a displacement time history with the Ricker wavelet shape, on a certain node. Amplitude, maximum frequency and

"t_0" parameter, characterising the Ricker wavelet shape, are introduced in the program with an appropriate input file.

In PEelse2D are also introduced some check routine:

- time step check, in order to satisfy the CFL (Courant-Friedrich-Levy) stability condition (Quarteroni, 2000);
- number of points per wavelength check, in order to correctly sampling up to a fixed frequency (tesi di laurea M. Da Prat).

6 Tests performed on a plane wave source

The following tests are performed in order to verify the correctness of the plane wave source implementation:

- numerical mesh (homogeneous domain) with plane wave load incidents on free surface normal direction;
- numerical mesh (homogeneous domain) with plane wave load incidents on free surface oblique direction;
- numerical mesh: elastic layer laying on an elastic half space.

6.1 Numerical mesh (homogeneous domain) with plane wave load incidents normal

First test performed on PEelse2D consists on the propagation of a plane wave source into an homogeneous domain, incidents normal the free surface. Mesh characteristics are shown in Fig. 1. For the special case of spectral degree equal to 4, we made use of a well tested criterion (Tesi di Laurea di M.Da Prat).

$$\Delta x_{macro} = \frac{V_S}{f_{\max}} \frac{4}{3} \qquad \text{Eq. 1}$$

Absorbing condition were not yet introduced at the time that the tests were performed. In order to avoid spurious reflection from the boundary, the mesh size is enlarged. This choice granted 8 sec. ((2000 m * 2) / 500 m/s) during which numerical and analytical solution must coincide.

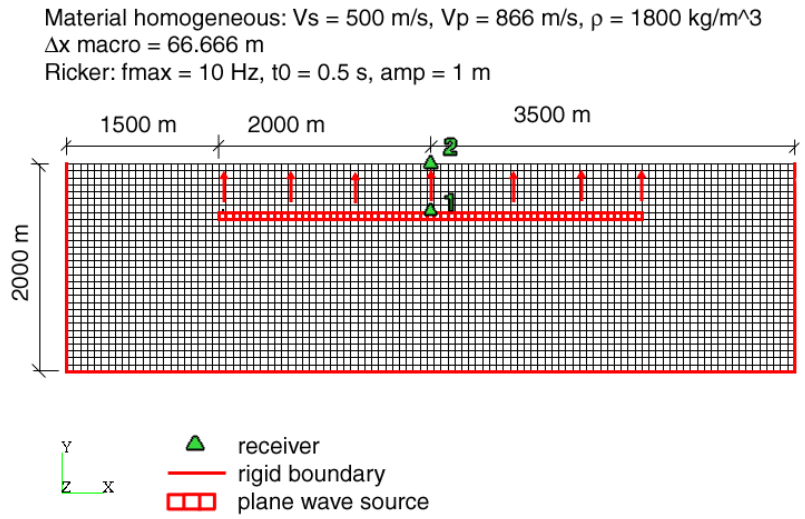

Fig. 1 – Numerical mesh (homogeneous domain) with plane wave load incidents on free surface normal direction.

Fig. 2a shows the comparison between theoretical solution (blue line) and analytical solution (red star), computed with PEelse2D. Receivers location is shown in Fig. 1: receiver 1 is placed very close to the plane wave generation area, while receiver 2 is located on the free surface and for this reason the maximum amplitude of the Ricker wavelet is twice the one monitored at receiver 1.

Moreover, Fig. 2a reports the L2 error (err L2), defined as the difference between analytical and numerical solution; this error reports, approximately, a value of 5%. Another important kind of error is the so called l2L2 (err l2L2), defined as the time integral of L2 error.

In order to obtain a term of comparison, we decided to reproduce the same test ran in the past on a numerical code of proven reliability: ELSE (Faccioli et al, 1997). Analysis is repeated with the numerical mesh previously described; the only difference is provided by the boundary conditions: rigid boundary is replaced with absorbing boundary conditions. This is decided for two reasons: reducing the computation time and resides on the numerical implementation of plane wave: ELSE plane wave source is located on the bottom element strip.

Fig. 2b shows the results of the numerical analysis; spectral degree is fixed to 4. L2 error is very close to the one shown in Fig. 2a, both in shape and amplitude.

First result of this analysis demonstrates that the chosen accuracy is not enough to allow a correct sampling of the input wave.

The analysis is repeated with a mesh as described in Fig. 1 except for spectral degree, increased to 5. Results obtained show a good improvement. Fig. 3a refers to results obtained with PEelse2D and Fig. 3b to the one obtained with ELSE.

a)

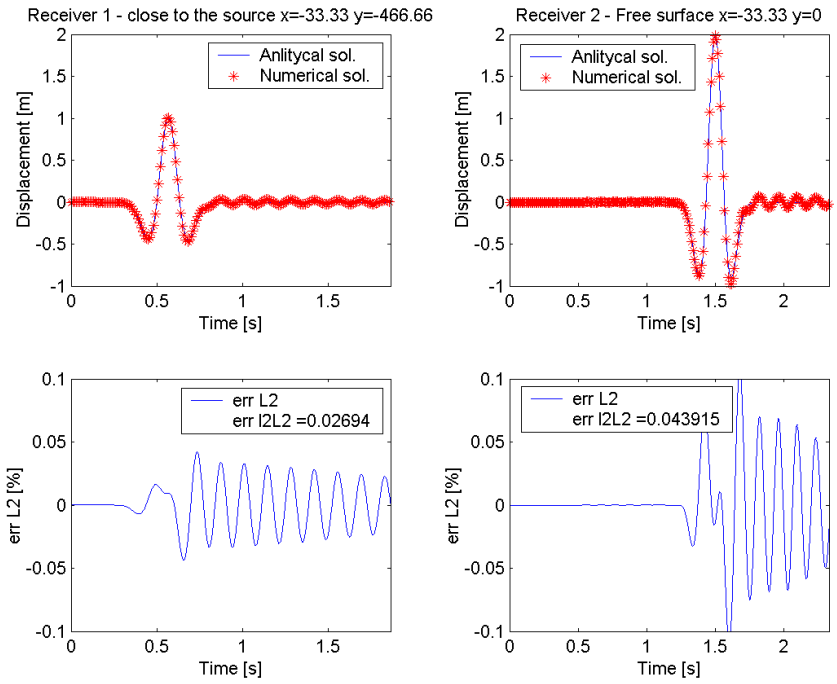

b)

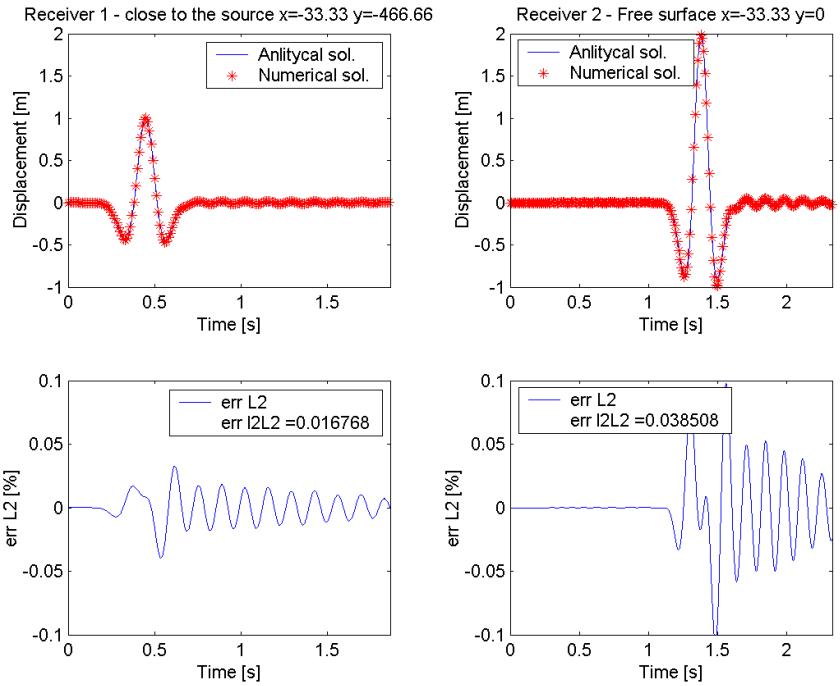

Fig. 2 – Recording obtained near the receivers **1** and **2**; first placed very close to the plane wave generation area, second on free surface (Fig. 1). Spectral degree 4. Fig. 2 a) shows the results obtained with the simulation performed with **PEelse2D**, while Fig. 2 b) shows the results obtained with the simulation performed with **ELSE**.

a)

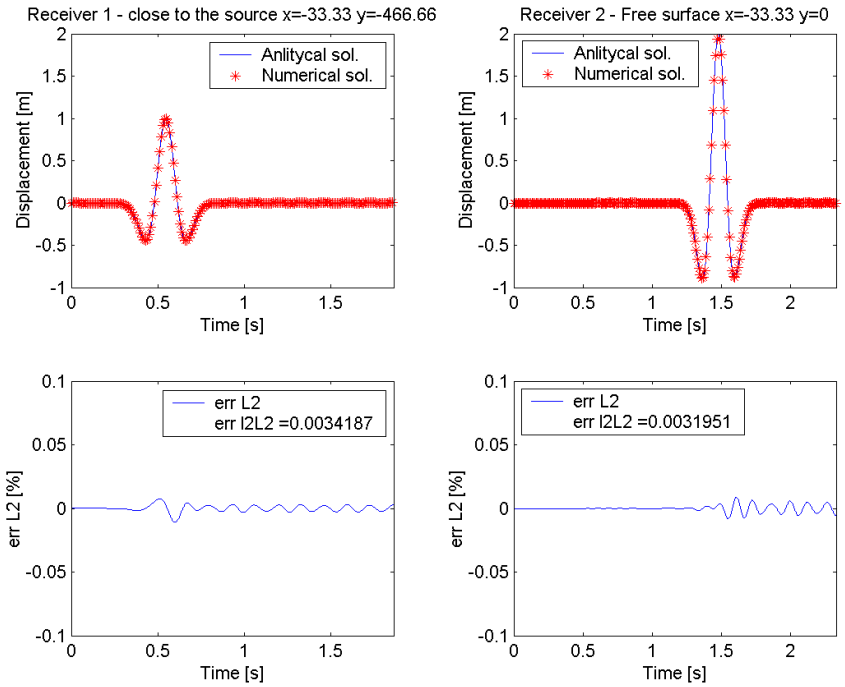

b)

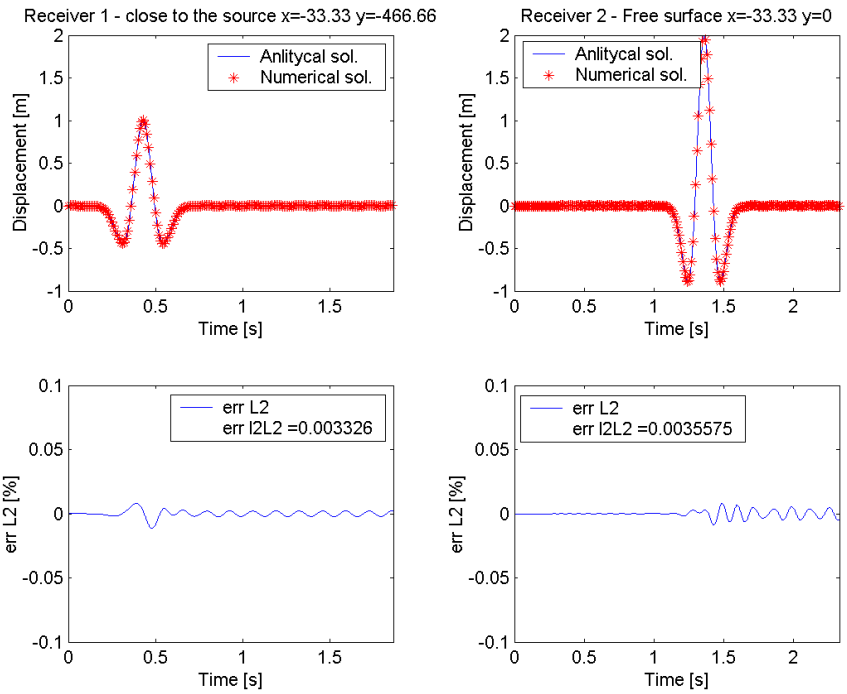

Fig. 3 –Recording obtained near the receivers **1** e **2**; first placed very close to the plane wave generation area, second on free surface (Fig. 1). Spectral degree 5. Fig. 3 a) shows the results obtained with the simulation performed with **PEelse2D**, while Fig. 3 b) shows the results obtained with the simulation performed with **ELSE**.

Returning to the issue of the dimensioning of the numerical mesh it is worth wile to note that Eq. 1 is based on the hypothesis that the integration nodes are equally spaced inside the spectral element; this hypothesis is false because the nodes are located on LGL positions. In order to achieve a more accurate evaluation of the number of sampling points per wavelength, it is decided to introduce inside PEelse2D an "ad hoc" procedure. This subroutine keeps into account the different length spacing between each node; it follows an example with spectral element of degree 4.

Fig. 4 shows the normalised position of LGL points for spectral degree 4.

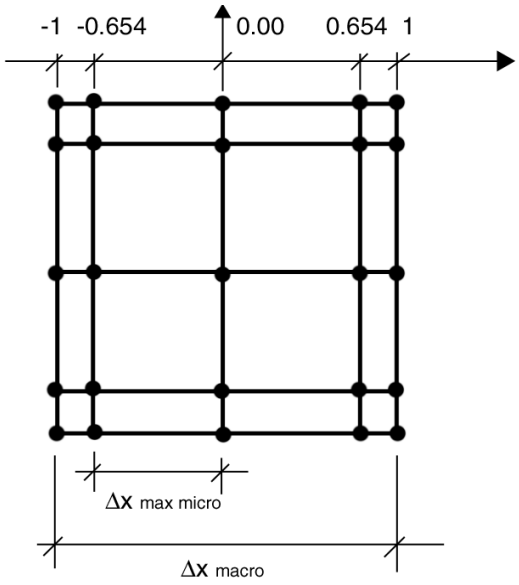

Fig. 4 – Position of LGL points for spectral degree 4.

Eq. 1 can be modified, exploiting the following proportion:

$$\frac{\Delta X_{macro}}{2} = \frac{\Delta X_{\max micro}}{0.654 - 0.00} \qquad \text{Eq. 2}$$

Finally:

$$\Delta X_{macro} = \frac{V_S}{f_{\max}} \left(\frac{2}{0.654} \right) \frac{1}{3} = \frac{V_S}{f_{\max}} \frac{3.058}{3} \qquad \text{Eq. 3}$$

Eq. 3 supplies a much more restrictive dimensioning of the mesh with respect to the one calculated with Eq. 1.

All these considerations are based on the hypothesis to have spectral degree equal to 4. Obviously, thanks to the capability of modifying the spectral degree of the mesh, it is possible to propose similar equation that gives the necessary number of points for a certain spectral degree, once that the wavelength is fixed.

In the following simulations it is provided to the correct sampling of the wavelength, adopting Eq. 3.

6.2 Numerical mesh (homogeneous space) with plane wave load incidents oblique

The second test provided concerns a numerical mesh (homogeneous space) with plane wave load incidents on free surface in oblique direction. Numerical mesh characteristics are shown in Fig. 5.

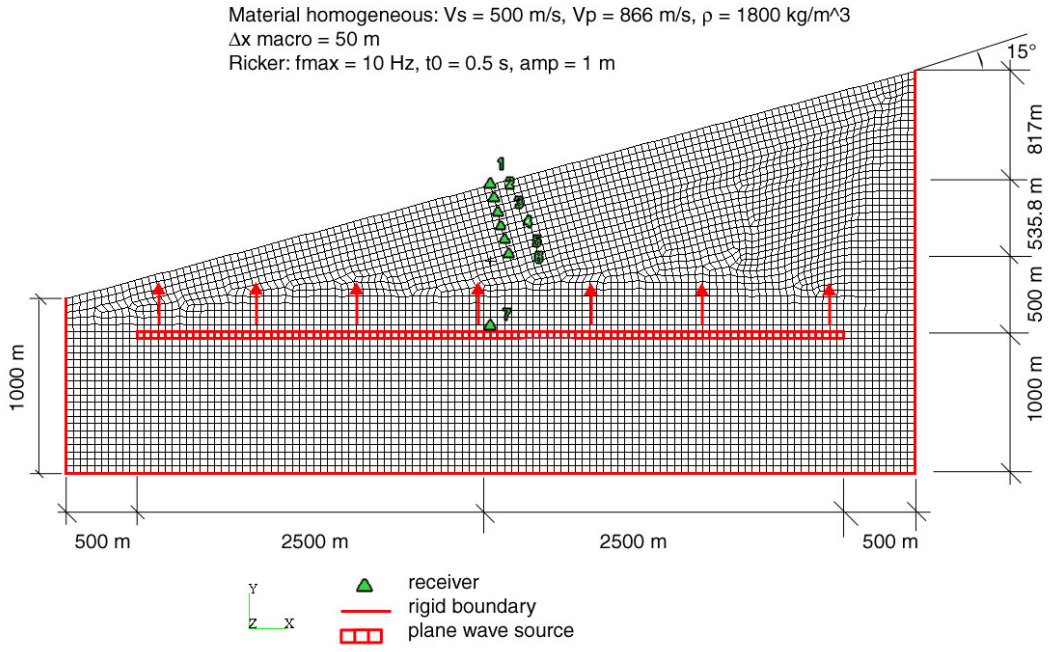

Fig. 5 – Numerical mesh (homogeneous space) with plane wave load incidents on free surface oblique direction.

Once more we provided the enlargement of the numerical mesh due to the lacking of absorbing conditions. Green triangles show the location of receivers. The comparison is performed thanks to the numerical program FREEFIELD (produced by Eng. M. Vanini), which computes the analytical solution for oblique wave propagation.

Fig. 6 shows displacement snapshot in horizontal direction (as in Fig. 5). The snapshots exhibit a good agreement with the analytical solution up to 3.5-4.0 seconds. Fig. 7 and Fig. 8 differ only for the spectral degree: 4 in Fig. 7 and 5 in Fig. 8.

Comparison between FREEFIELD (red line) and PEelse2D (green line) looks like very satisfactory for the receivers from 1 to 6. Displacement time history obtained in receiver 7 is altered by the reflection coming from the border at approximately 4 sec. Beyond this limit the simulation loses significance. Comparison between Fig. 7 and Fig. 8 shows that Eq. 3 gives a correct sampling avoiding any visible lost of accuracy both with spectral degree 5 to 4.

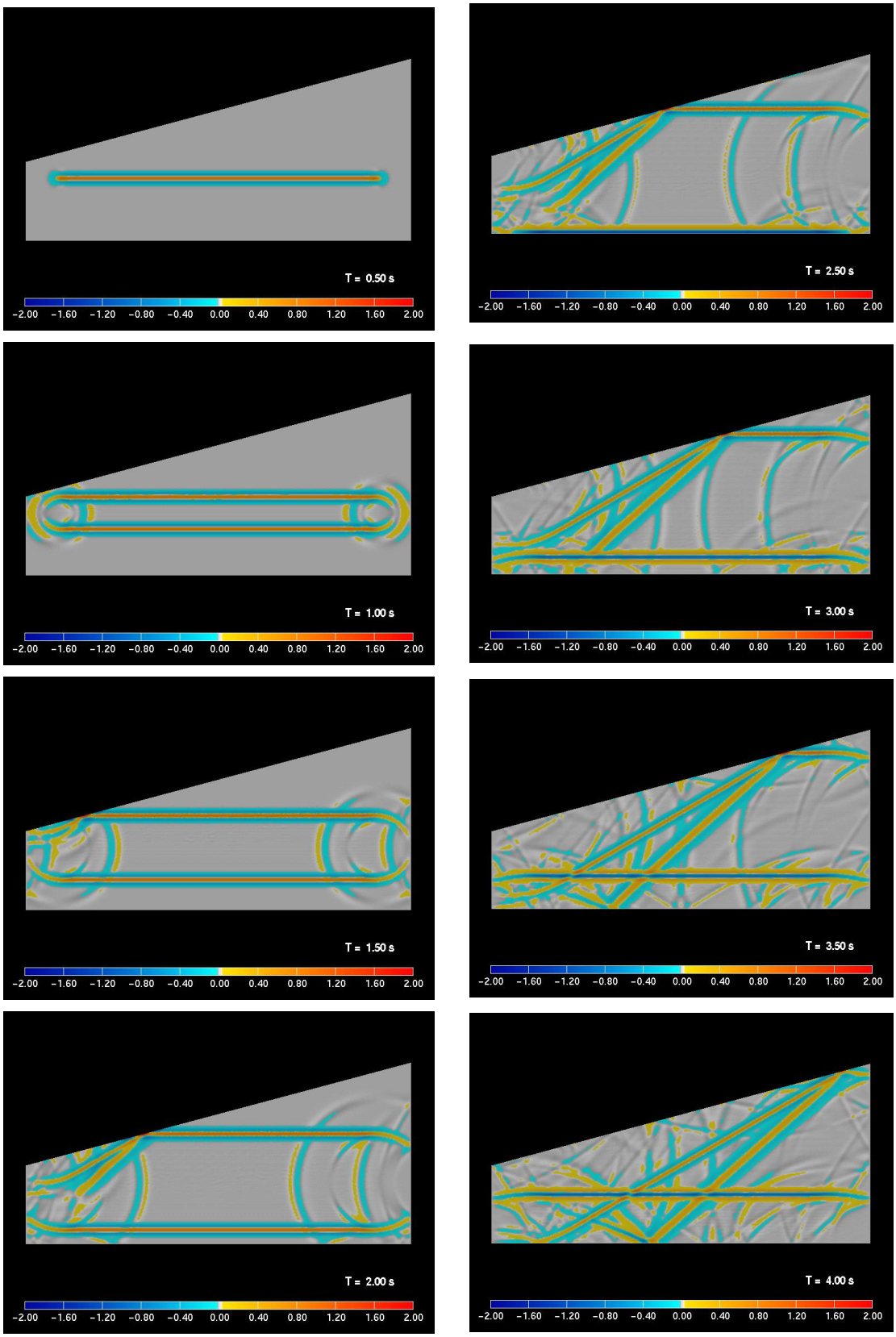

Fig. 6 – Displacement snapshot in horizontal direction in mesh of Fig. 5) with plane wave load incidents on free surface oblique direction. Shear wave propagates in direction y. Analysis spectral degree equal to 4.

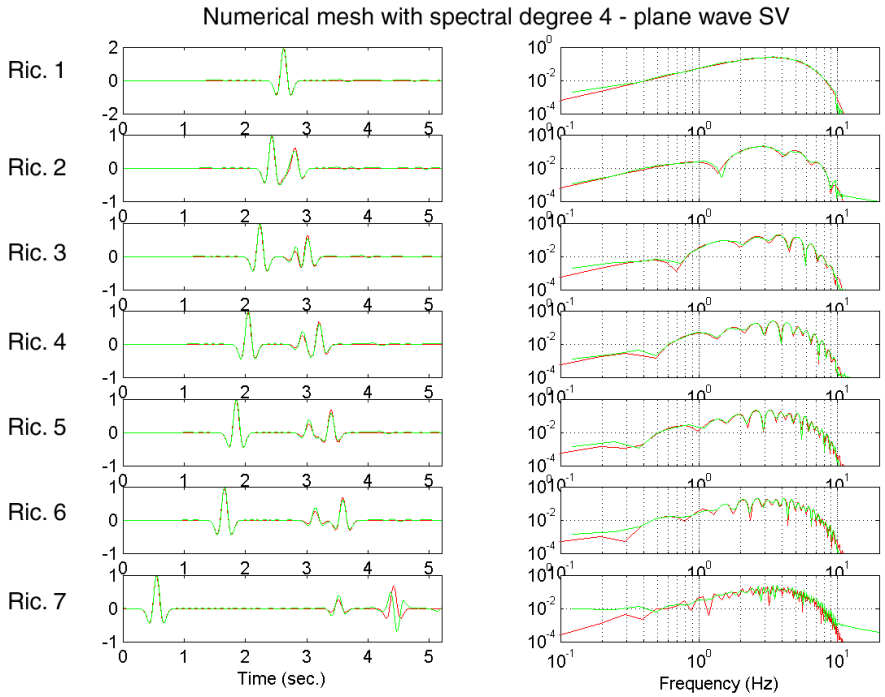

Fig. 7 – Comparison between FREEFIELD (red line) and PEelse2D (green line). SV wave (displacement in horizontal direction) propagates into the mesh of Fig. 5 (with spectral degree 4) along direction y.

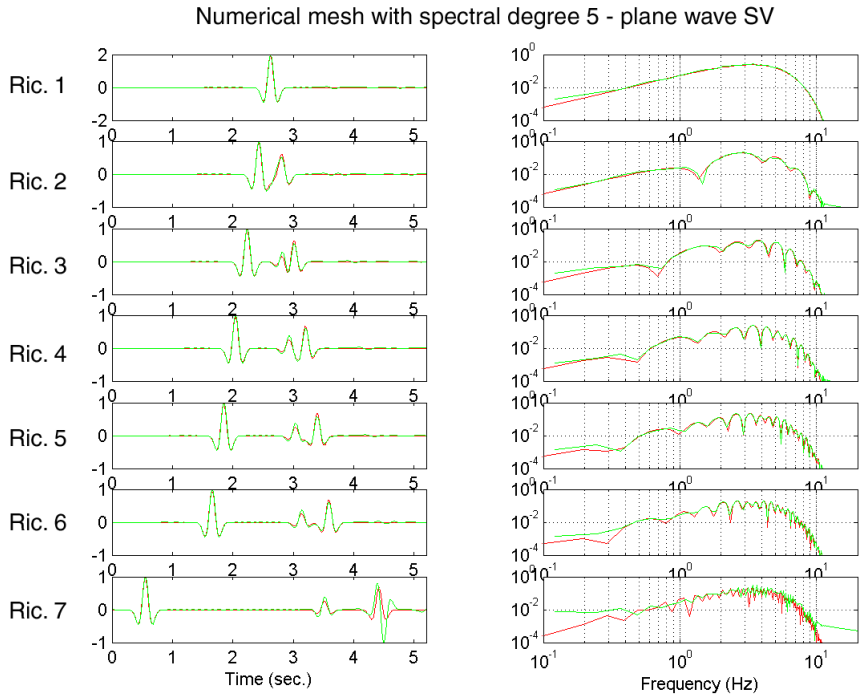

Fig. 8 – Comparison between FREEFIELD (red line) and PEelse2D (green line). SV wave (displacement in horizontal direction) propagates into the mesh of Fig. 5 (with spectral degree 5) along direction y.

6.3 Numerical mesh (horizontal layer laying on a half space) with plane wave load incident on normal direction

Last test is performed on a numerical mesh described as “elastic layer laying on an elastic half space” with plane wave load incidents on normal direction. Fig. 9 shows numerical mesh characteristics.

The solution provided by the Macro Excel EERA (calculation performed in the frequency domain - http://geoinfo.usc.edu/gees/Software/EERA2000/Default.htm) is compared with the displacement time history on the surface node 1 (Fig. 10).

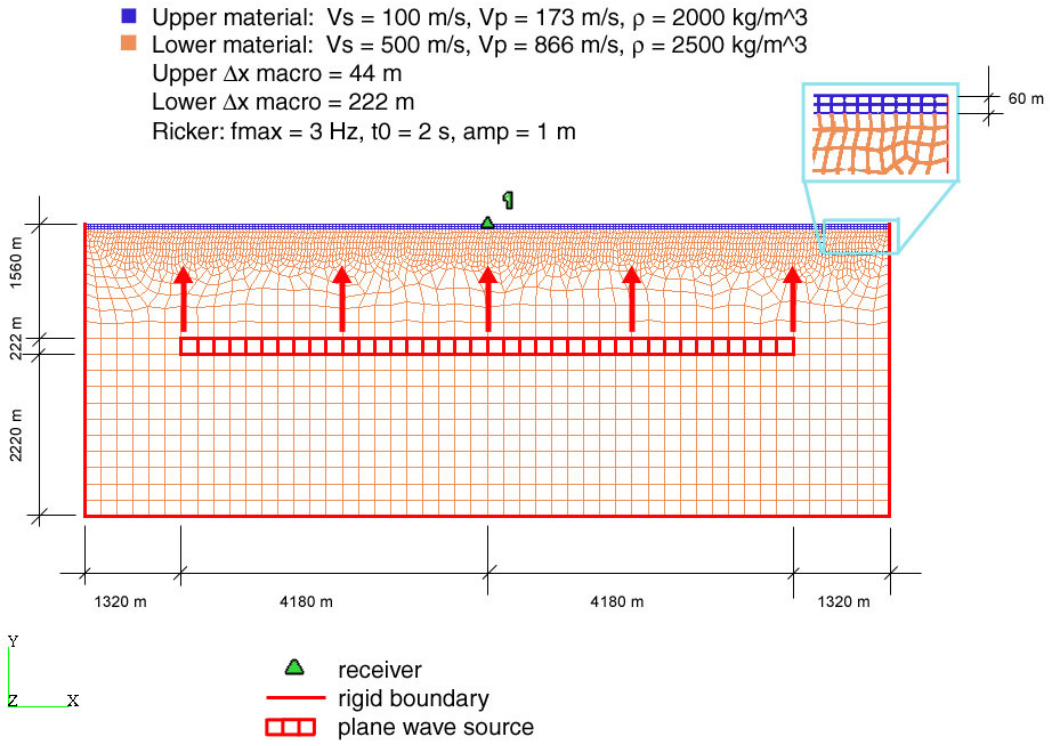

Fig. 9 – Numerical mesh “elastic layer laying on an elastic half space” with plane wave load incidents on normal direction.

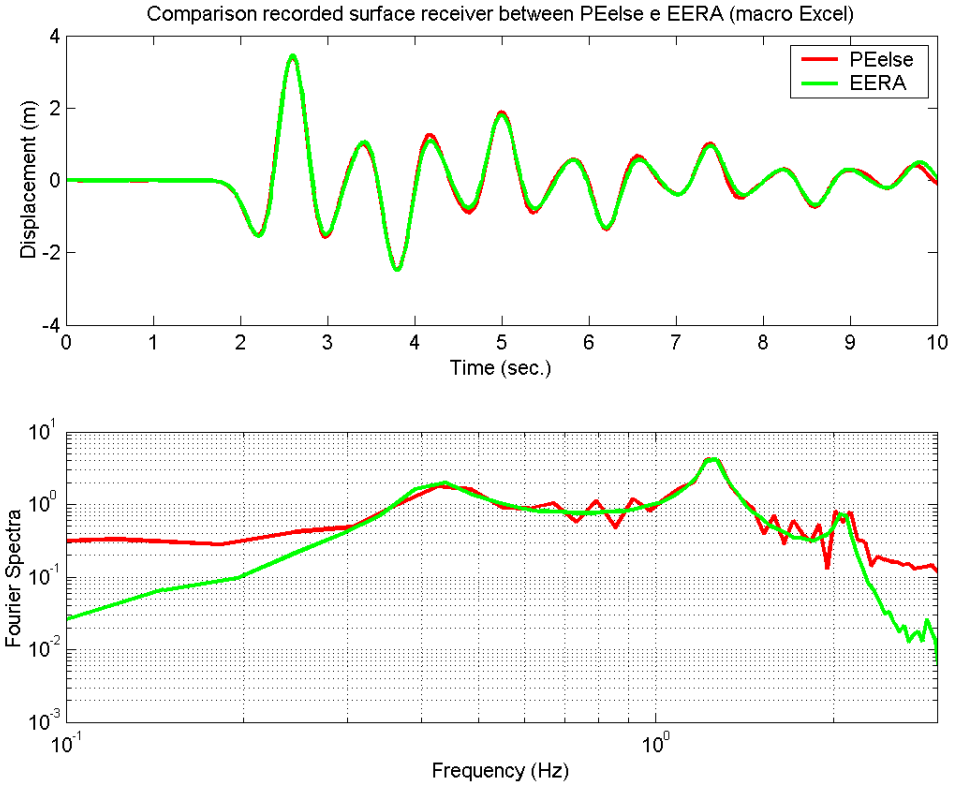

Fig. 10 – Displacement time history at node 1, for the simulation of the numerical mesh "elastic layer laying on an elastic half space" with plane wave load incidents on normal direction, as described Fig. 9.

7 Absorbing boundary conditions

A customary approach for dealing with infinite media consists of introducing a fictitious boundary and setting absorbing conditions on it. We present limit ourselves to first order conditions; the so-called P3 paraxial conditions due to Stacey (1988) are adopted in PEelse2D. Stability is ensured for Poisson coefficient $\nu \leq 0.333$, approximately.

Fig. 11 shows the numerical domain excited by plane shear-wave (Ricker wavelet shape) load incidents on upper edge normal direction and P3 paraxial conditions enforced on the four side.

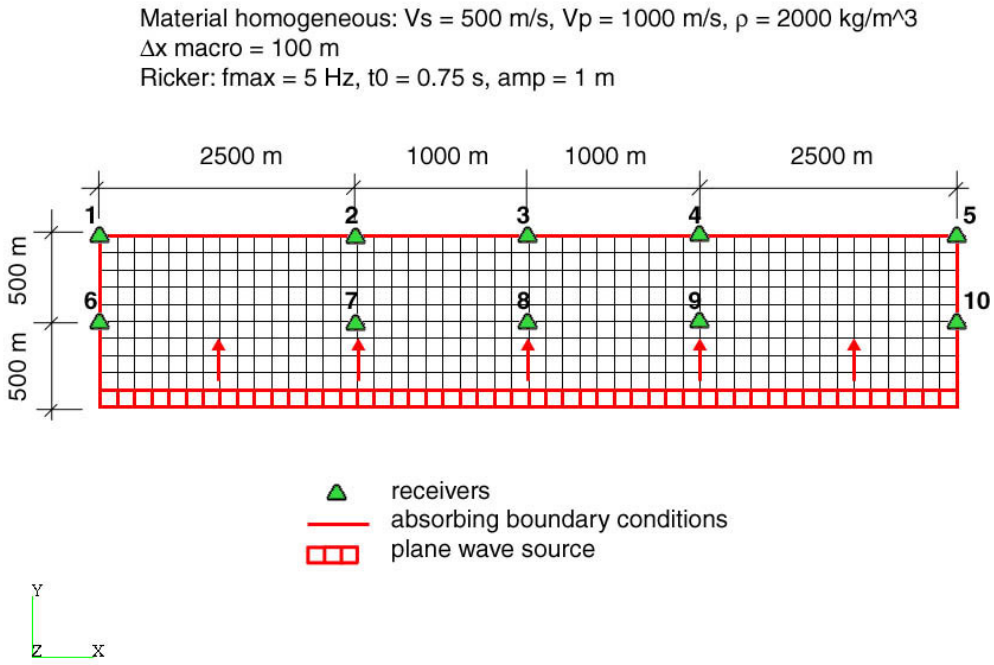

Fig. 11 – Numerical mesh (unbounded homogeneous space) with plane shear-wave load incidents on upper edge normal direction.

We proceed like in §6.1. Analysis are both performed on ELSE and PEelse2D to obtain a term of comparison. Fig. 12 shows the comparison between recorded displacement time history for ELSE simulation (green dotted line) and for PEelse2D simulation (red line). Results testifies that ELSE accuracy is granted also on PEelse2D.

a)

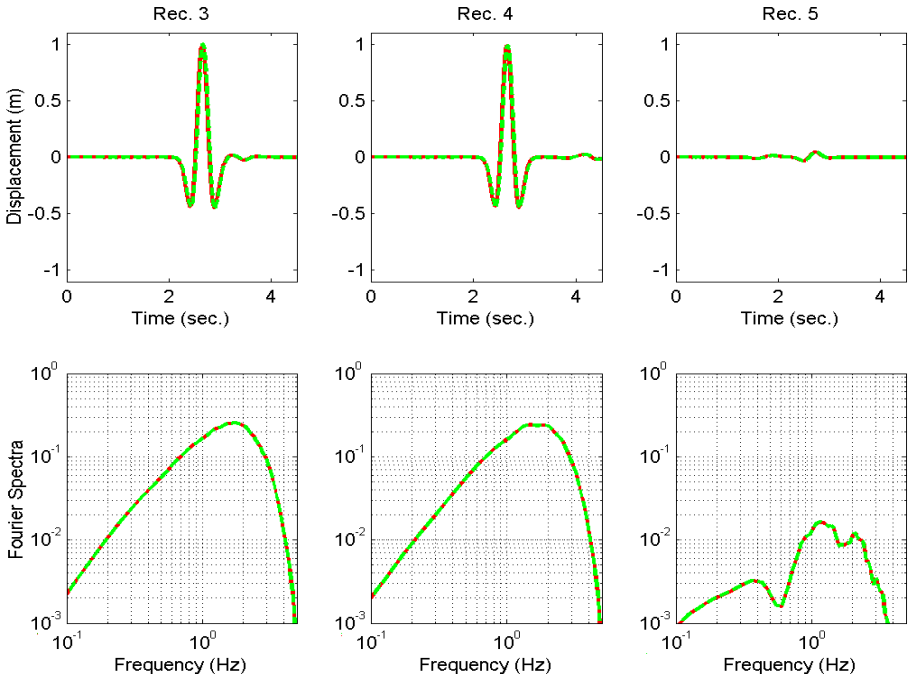

b)

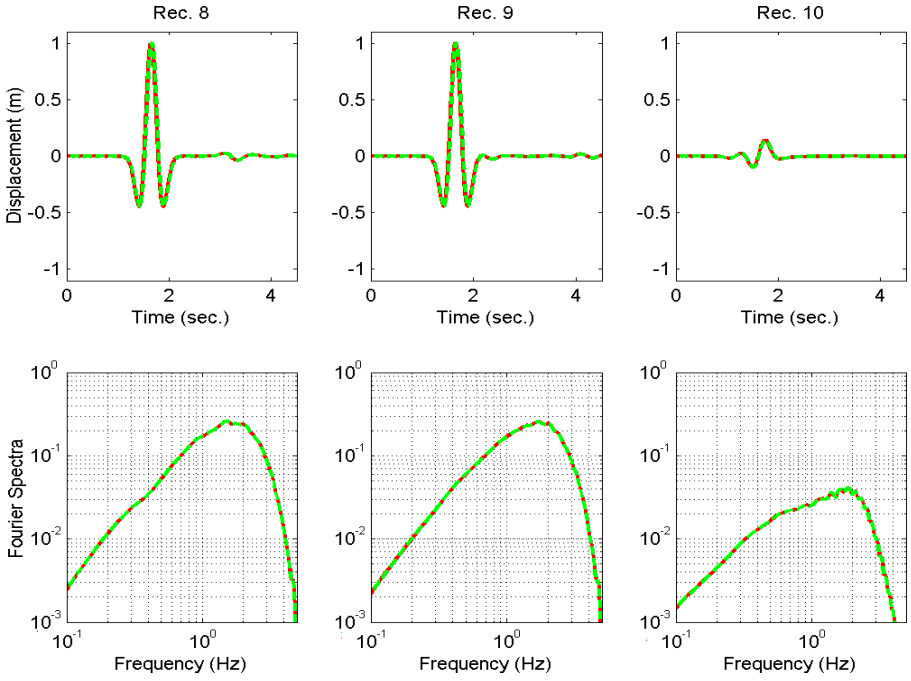

Fig. 12 – Comparison between recorded horizontal displacement time history at different nodes of mesh described in Fig. 11. **Green dotted line**: time history produced by ELSE; **red line**: time history produced by PEelse2D.

Fig. 13 shows displacement snapshots from 1 up to 9 seconds in horizontal direction. Test has been performed on an unbounded homogeneous domain characterised by density $\rho = 2000\ kg/m^3$, and propagation velocities $V_P = 1000\ m/s$ and $V_S = 500\ m/s$. Excitation is a concentrated horizontal force impulse with peak frequency $f_P = 5\ Hz$ and unit peak amplitude in time domain. After 8.5 seconds there are no more wave propagating on the control domain.

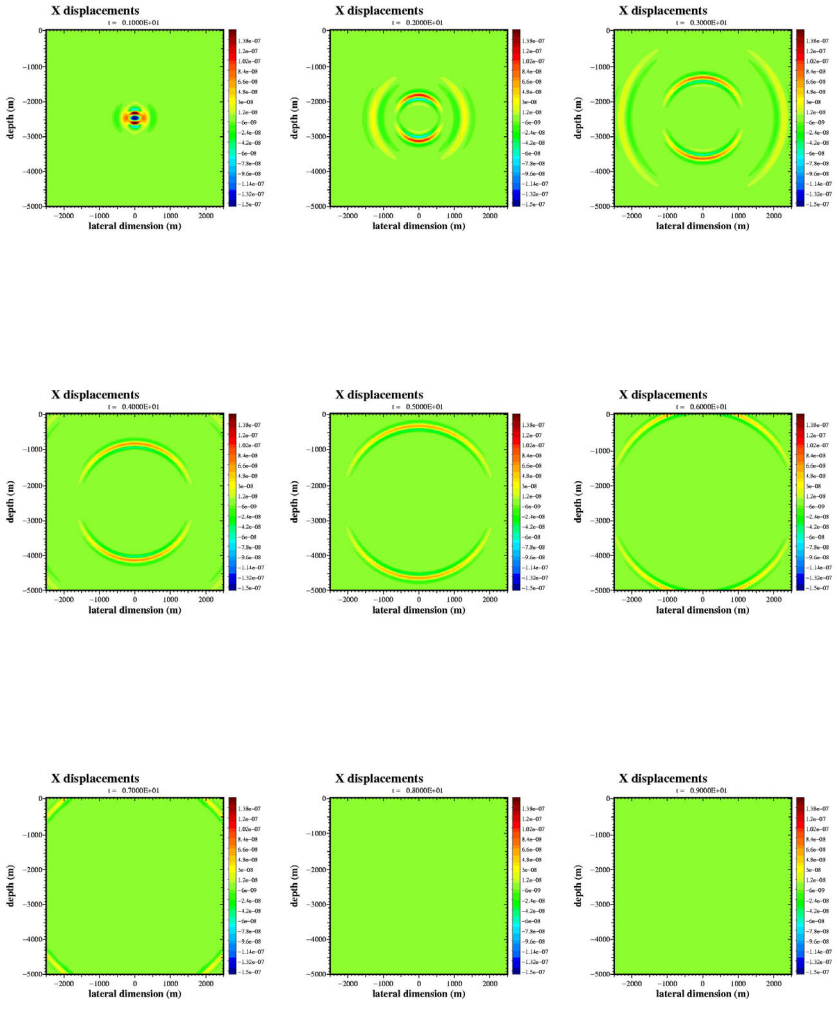

Fig. 13 – Displacement snapshots from 1 up to 9 seconds in horizontal direction. Homogeneous unbounded mesh is excited by point load force.

8 Seismic moment

A major research interest in seismology is the description of the physics of the seismic sources. In PEelse2D moment seismic source and fault are introduced as described by Madariaga (1983). Tests performed by Eng. P. Parla (Tesi di Laurea, P.Parla) are reproduced.

8.1 Seismic moment point source

As a first test problem, we consider a seismic moment point source excitation in an unbounded homogeneous domain characterised by density $\rho = 2500\ kg/m^3$, and propagation velocities $V_P = 5700\ m/s$ and $V_S = 3420\ m/s$. Time-dependent part of the impulse is a Ricker wavelet with peak frequency $f_P = 1\ Hz$ and unit peak amplitude in time domain.

The first order P3 paraxial conditions were enforced on the four side of the computational grid, consisting of 784 subdomains 1 km × 1 km in size (Fig. 14a). Fig. 14b shows the unstructured mesh, that is created to verify the correct implementation of seismic source on an unstructured domain.

Fig. 15 shows the comparison between recorded displacement time history between ELSE (left side – black line) and PEelse2D (right side; structured mesh – red line and unstructured mesh – green dotted line). Meshes described in Fig. 14 are excited by seismic moment point source (dip-slip 90°). Comparison shows identical time history recorded on all three numerical simulations.

Same kind of comparison is performed in Fig. 16, where meshes, described in Fig. 14, are now excited by seismic moment point source (dip-slip 45°).

a)

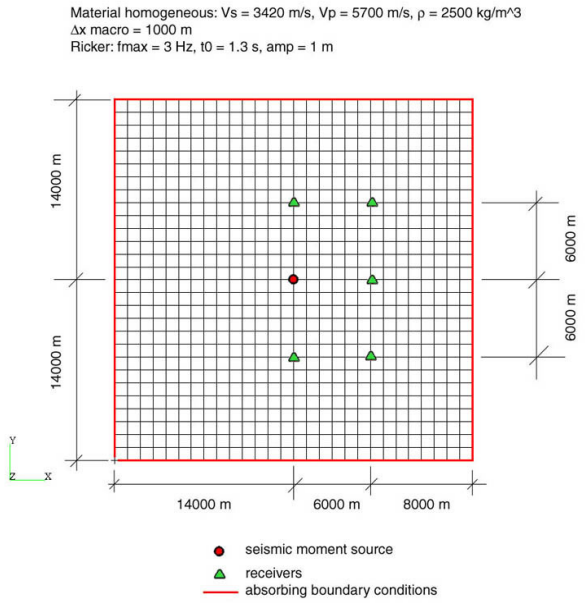

b)

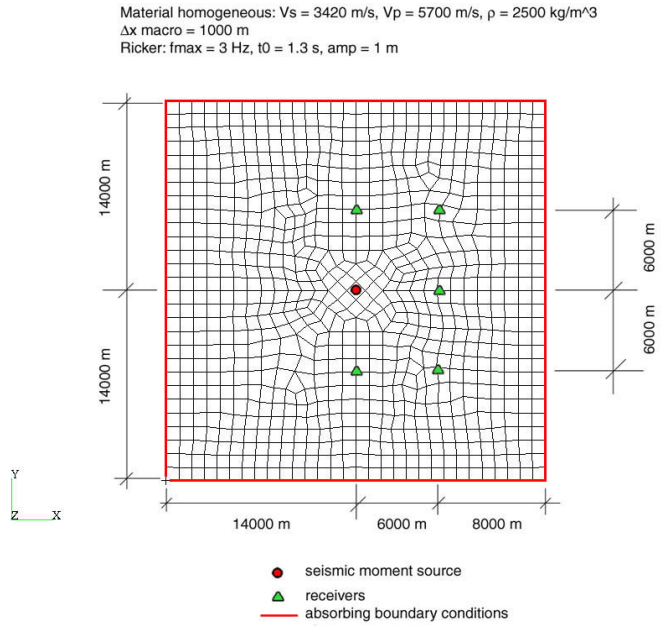

Fig. 14 – Numerical mesh (homogeneous unbounded domain) with seismic moment point load excitation. **a)** structured mesh; **b)** unstructured mesh.

HORIZONTAL DISPLACEMENT

ELSE

PEelse2D
(structured and unstructured)

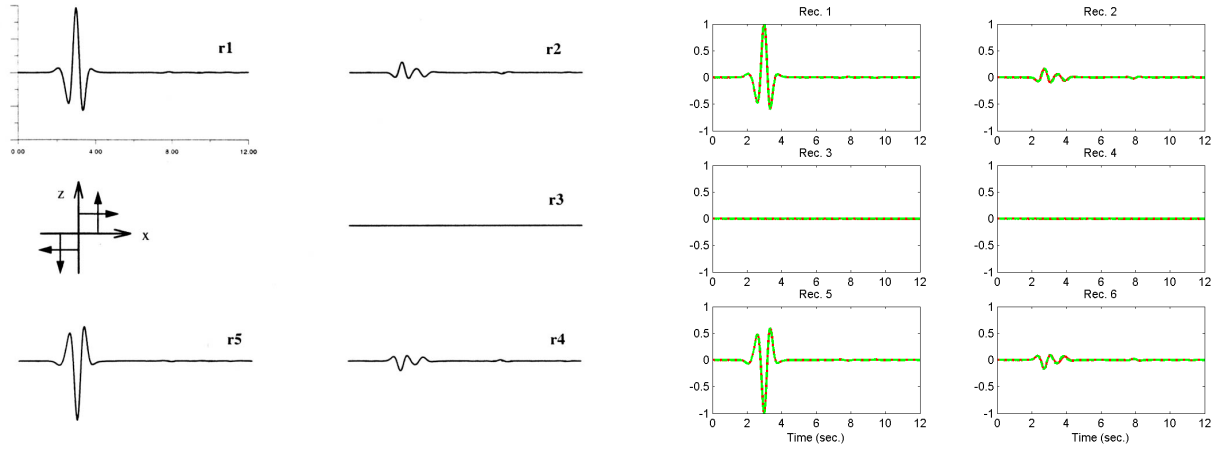

VERTICAL DISPLACEMENT

ELSE

PEelse2D
(structured and unstructured)

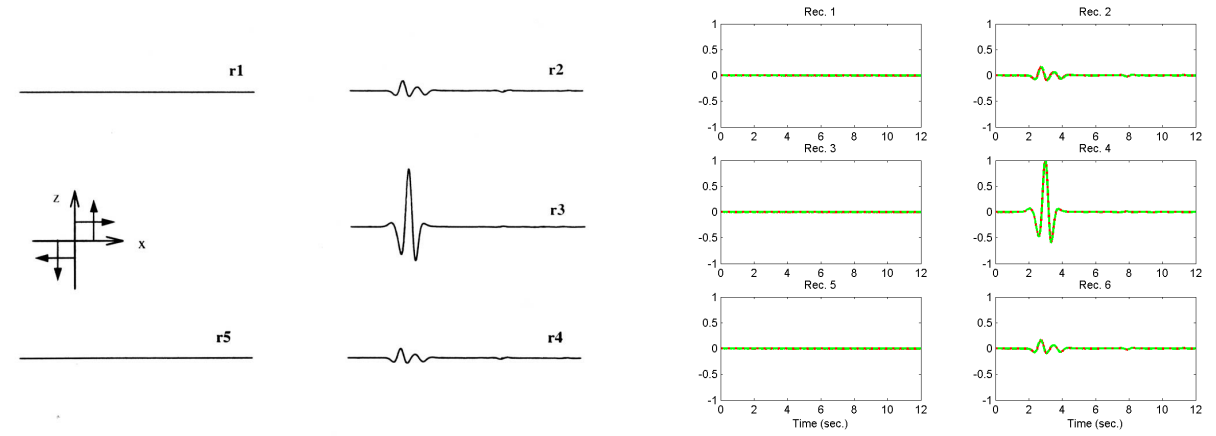

Fig. 15 – Comparison on recorded displacement time history between ELSE (left side – black line) and PEelse2D (right side; structured mesh – red line and unstructured mesh – green dotted line). Seismic moment point source (dip-slip 90°)

HORIZONTAL DISPLACEMENT

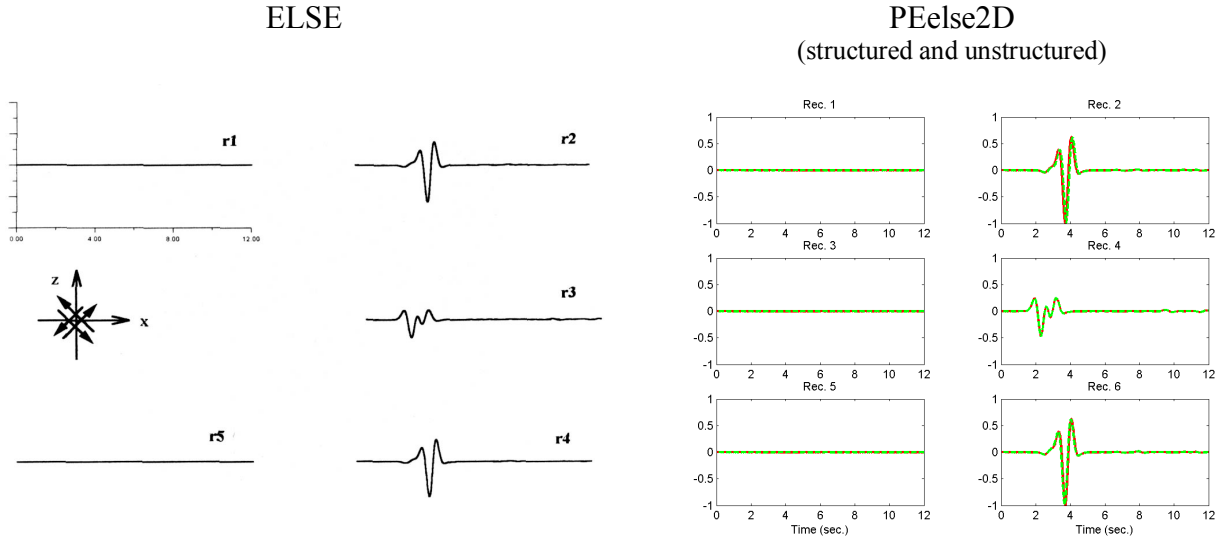

VERTICAL DISPLACEMENT

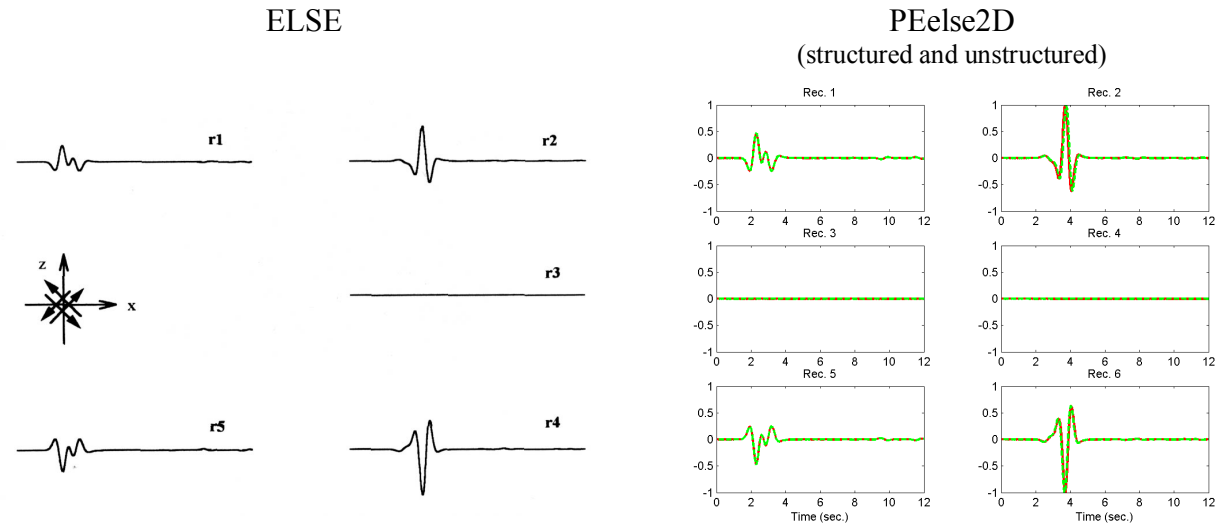

Fig. 16 – Comparison on recorded displacement time history between ELSE (left side – black line) and PEelse2D (right side; structured mesh –red line and unstructured mesh – green dotted line). Seismic moment point source (dip-slip 45°)

8.2 Vertical fault

A second series of test were performed on the fault source. Unbounded homogeneous domain consists of 784 subdomains 1 km × 1 km in size (Fig. 17). Fig. 18 shows the comparison between recorded displacement time history between ELSE (left side – black line) and PEelse2D (right side; structured mesh –red line and unstructured mesh – green dotted line).

Mesh described in Fig. 17 is excited by vertical fault and the time-dependent part of the impulse is a Ricker wavelet with peak frequency $f_P = 1\ Hz$ and unit peak amplitude in time domain. Comparison shows the identical time history recorded on all three numerical simulations.

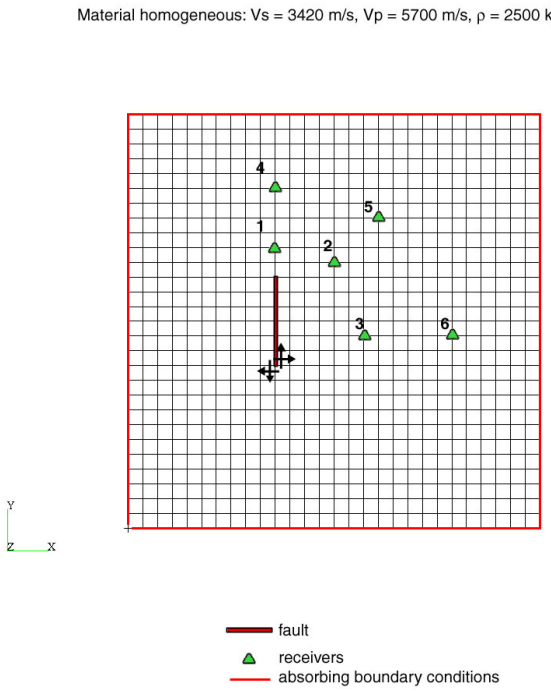

Fig. 17 – Numerical mesh (homogeneous unbounded domain) with vertical fault excitation.

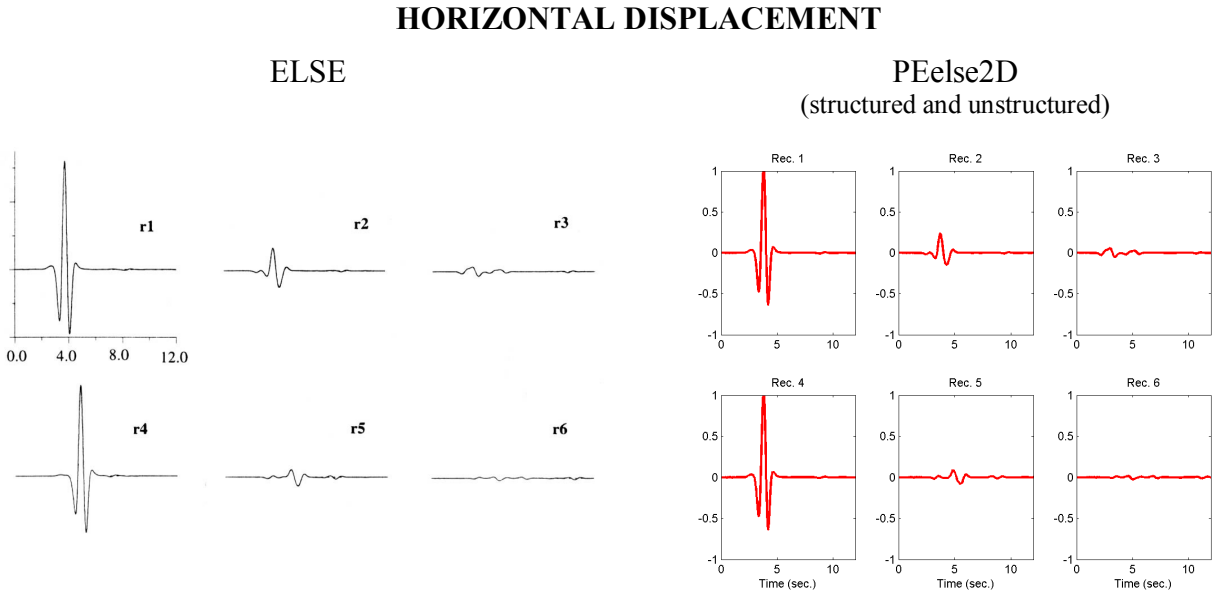

Fig. 18 – Comparison on recorded displacement time history between ELSE (left side – black line) and PEelse2D (right side; structured mesh –red line and unstructured mesh – green dotted line). Vertical fault excitation.

8.3 Oblique fault

Last test is performed on homogeneous unbounded domain excited by an oblique fault, as described in Fig. 19a and Fig. 19b. The first (Fig. 19a) is identical to previous mesh test (Fig. 17), while the second (Fig. 19b) has the same physical characteristics ($\rho = 2500\ kg/m^3$, $V_P = 5700\ m/s$ and $V_S = 3420\ m/s$) but the grid is unstructured. Spectral element surrounding the oblique fault must have the same dimension, in order to evaluate correctly the seismic moment tensor density m_{ij} (Tesi di Laurea, P. Parla).

Fig. 20 shows the comparison between recorded displacement time history between ELSE (left side – black line) and PEelse2D (right side; structured mesh –red line and unstructured mesh – green dotted line).

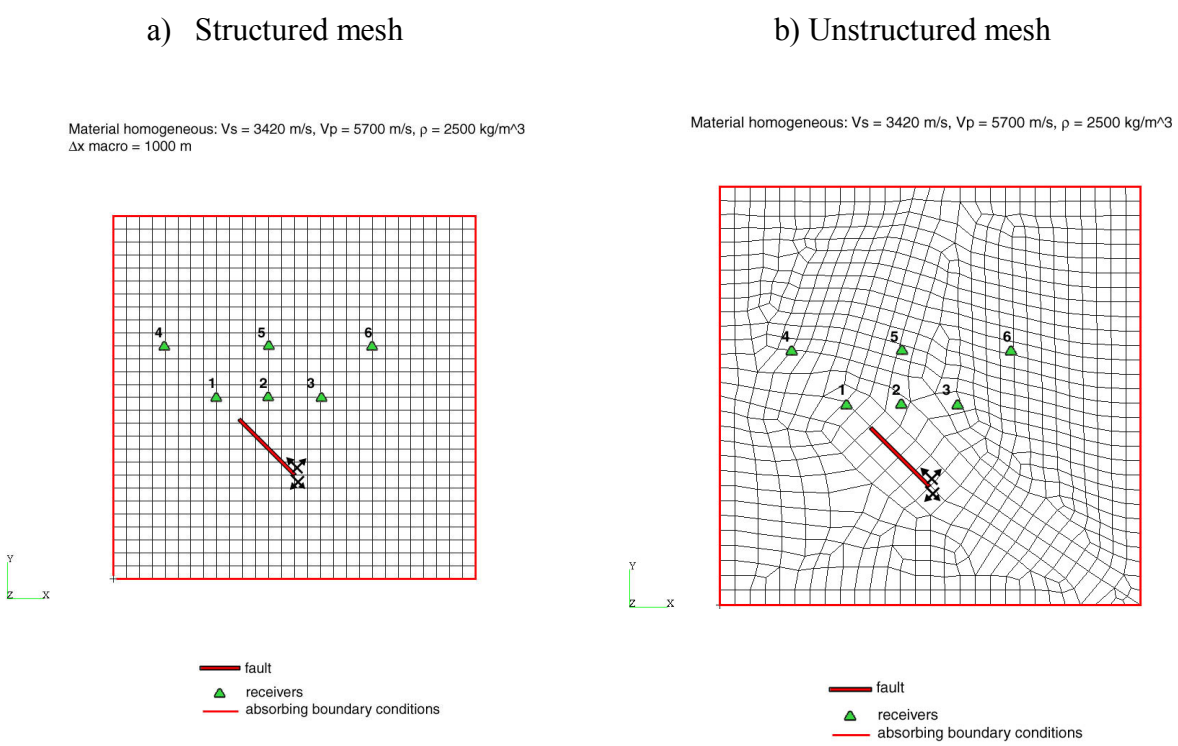

Fig. 19 – Numerical mesh (homogeneous unbounded domain) with oblique fault excitation (45°). **a)** structured mesh; **b)** unstructured mesh.

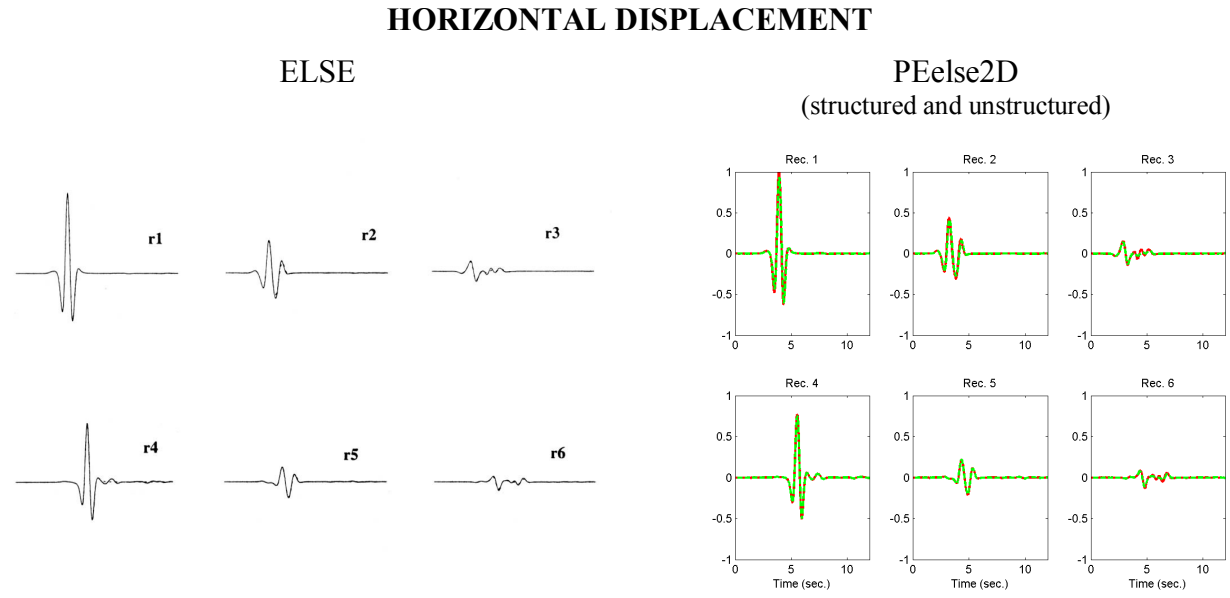

Fig. 20 – Comparison on recorded displacement time history between ELSE (left side – black line) and PEelse2D (right side; structured mesh –red line and unstructured mesh – green dotted line). Oblique fault excitation.

9 Internal soil dissipation

Internal soil dissipation has been introduced in the code as described by Kosloff and Kosloff (1986). Fig. 21 shows the characteristics of the unbounded homogeneous domain chosen for the test. We consider a plane shear-wave load incidents on upper edge normal direction.

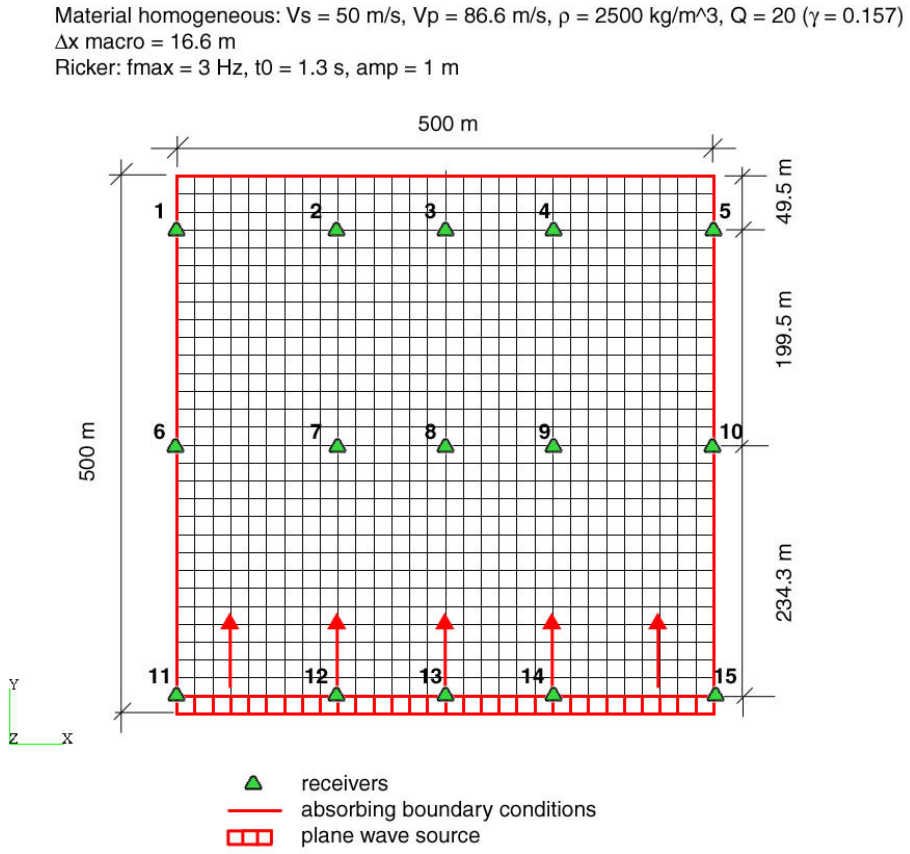

Fig. 21 – Numerical mesh (unbounded homogeneous domain) with plane shear-wave load incidents on upper edge normal direction.

Fig. 22 shows displacement snapshots at 1.3, 6.0 and 10 seconds in horizontal direction on mesh of Fig. 21. On left side no damping is introduced in the material., while, on the right side, internal soil dissipation is introduced with the following parameters: $Q_0 = 20, f_0 = 1\ Hz$ and $\gamma = 0.157$.

Finally Fig. 23 shows the comparison between recorded horizontal displacement time history at different nodes of mesh described in Fig. 21 with no damping (green dotted line) and with internal soil dissipation (red line).

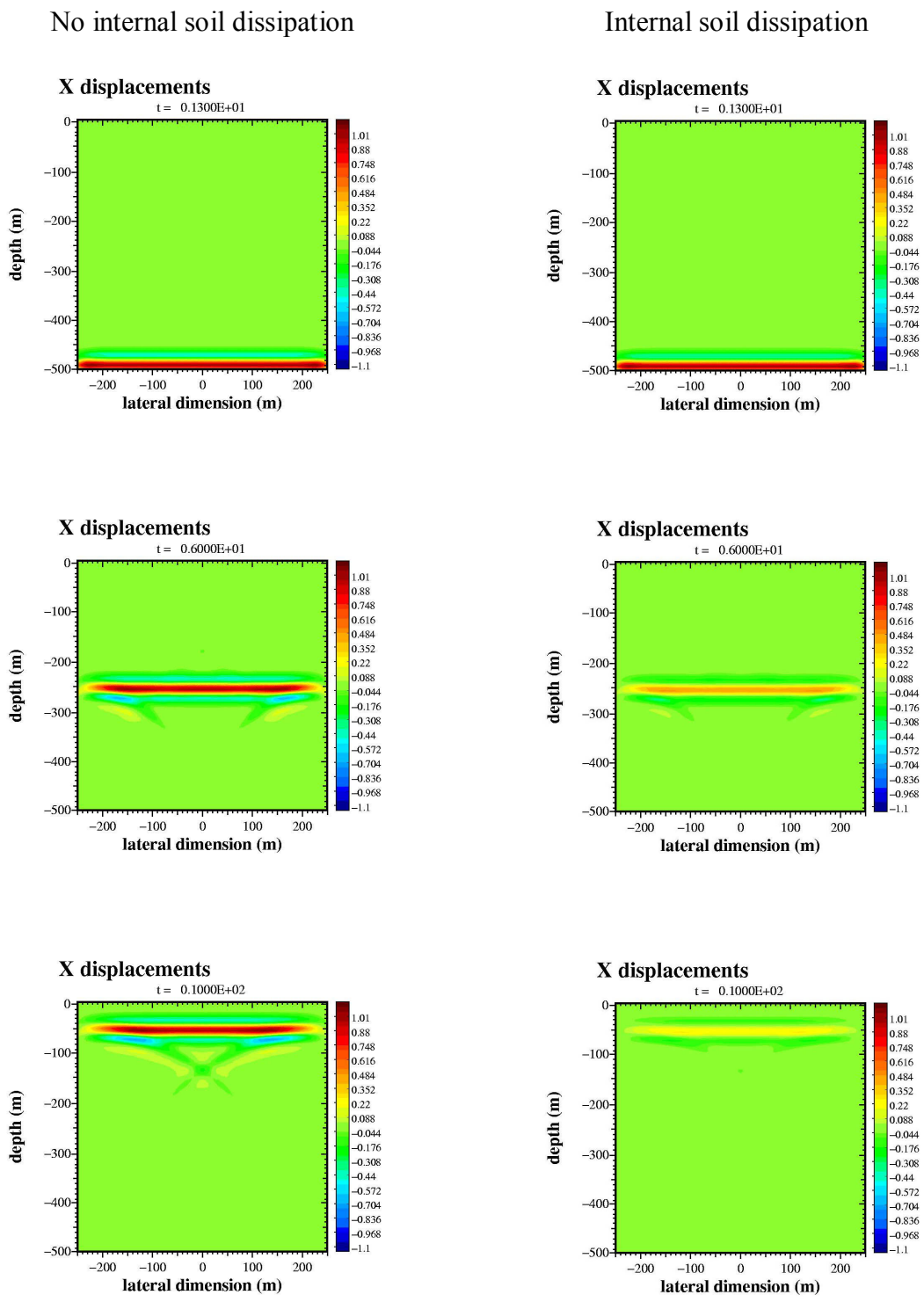

Fig. 22 – Displacement snapshots at 1.3, 6.0 and 10 seconds in horizontal direction on mesh of Fig. 21. Plane shear-wave load incidents on free surface normal direction. **Left side** – no damping is introduced in the material. **Right side** – internal soil dissipation introduced as described by Kosloff and Kosloff (1986*); $Q_0 = 20, f_0 = 1\ Hz$* and $\gamma = 0.157$. Analysis spectral degree equal to 4.

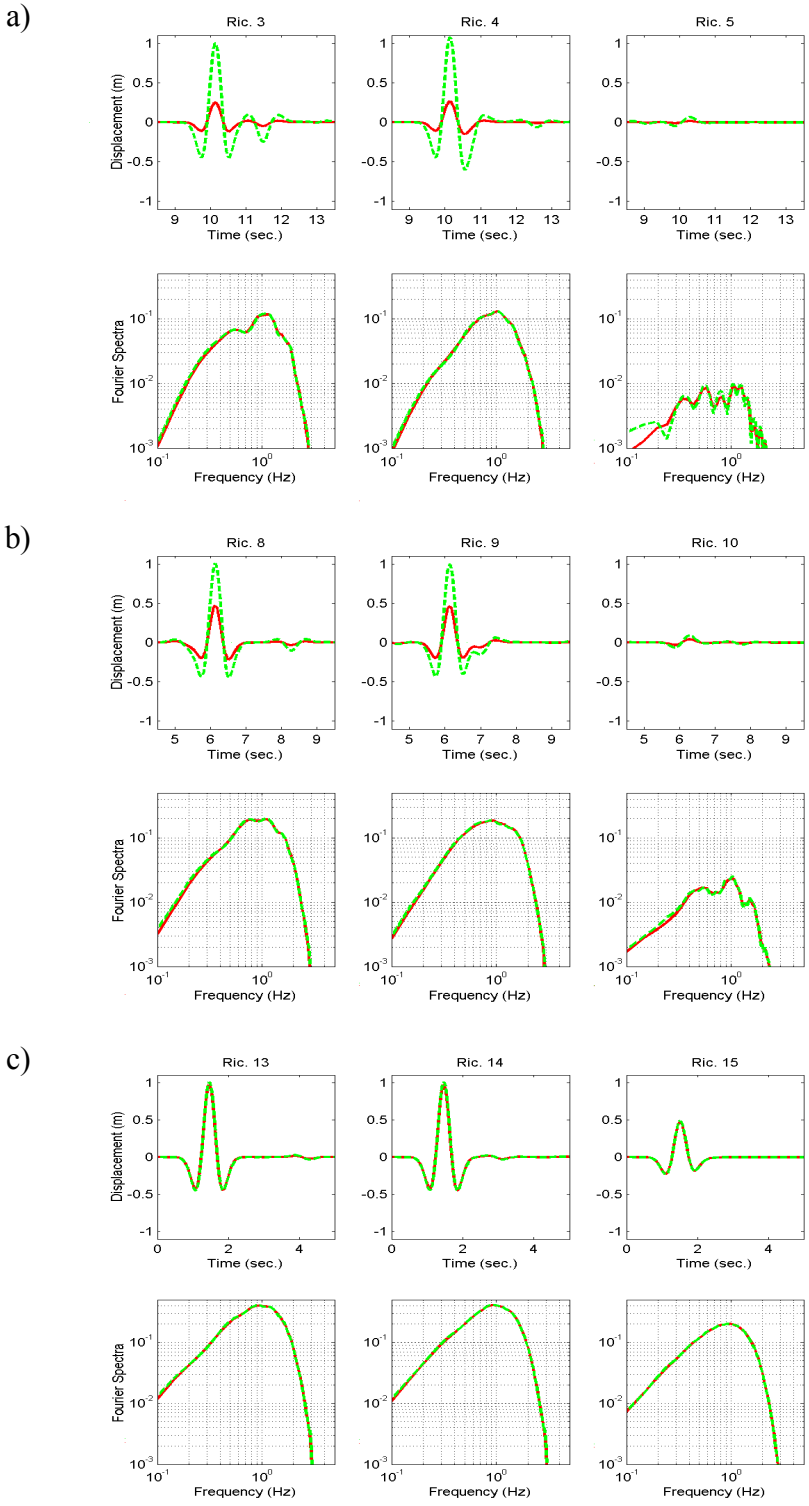

Fig. 23 – Comparison between recorded horizontal displacement time history at different nodes of mesh described in Fig. 21 with no damping (green dotted line) and with internal soil dissipation (red line).

10 Further development on PEelse2D

Final period will concern the following topics:

- verifying the correct behaviour of absorbing boundary conditions; reproducing different tests already performed within the AHNSE program validation;
- accurate test on both seismic moment tensor and fault;
- accurate test on internal soil dissipation;
- writing “user manual” for PEelse2D;
- writing “how to - guide” with some examples of analysis performed with PEelse2D;
- producing a “benchmark library” of test cases with analytical solution in order to subject program modifications to automatic validation.

11 Bibliography

Casadei, F., and Gabellini, E. (1997) – *"Implementation of a 3D coupled Spectral Element solver for wave propagation and soil-structure interaction simulations"*. European Commission Joint Research Center Report EUR17730EN;

Da Prat, M. (1996) – *"Applicazione dei metodi spettrali al calcolo della risposta sismica locale"*. Tesi di Laurea in Ingegneria Civile per la Difesa del Suolo e la Pianificazione Territoriale, Politecnico di Milano;

Faccioli, E., Maggio, F., Paolucci, R., and Quarteroni, A. (1997) – *"2D and 3D elastic wave propagation by a pseudo-spectral domain decomposition method"*. J. Seismology, **1**, 237–251;

Kosloff, R., and Kosloff, D. (1986) – *"Absorbing boundaries for wave propagation problems"*. J. Comp. Phys., 63, 363-376;

Madariaga, R. (1983). – *"Earthquake source theory: a review, in H. Kanamori and E. Boschi (eds.), Earthquakes: Observation, Theory and Interpretation"*. North Holland Publishing Company, Amsterdam, 1-44;

Parla, P. (1997) – *"Modellazione della sorgente sismica in 2D in un algoritmo pseudo-spettrale"*. Tesi di Laurea in Ingegneria Civile per la Difesa del Suolo e la Pianificazione Territoriale, Politecnico di Milano;

Quarteroni, A. (2000) – *"Modellistica Numerica per Problemi Differenziali"*. Springer Italia;

Stacey, R. (1988) – "*Improved transparent boundary formulations for the elastic wave equations*". Bulletin of the Seismological Society of America, 78, 2089-2097.